Reaction Kinetics of a Selected Number of Elementary Processes Involved in the Thermal Decomposition of 9-Methylphenanthrene Using Density Functional Theory

Theodorus J. M. de Bruin,[†] François Lorant,*,[†] Hervé Toulhoat,[†] and William A. Goddard III[‡]

Institut Français du Pétrole, 1-4 Avenue de Bois Préau, 92852 Rueil-Malmaison Cedex, France, and Material Simulation Center, Beckman Institute (139-74), California Institute of Technology, Pasadena, California 91125

With the use of general transition state theory and density functional theory, six reference reactions that are thought to play an essential role in the thermal cracking process of 9-methylphenanthrene have been studied. At the uB3LYP/6-31G(d,p) level, the transition state structures could be located on the 0 K potential energy surface for the three propagation reactions which induce no net creation/annihilation of radicals, and the calculated activation energies and preexponential frequency factor generally correspond well to experimental values. The transition states for two termination reactions were determined by replacement of a phenanthrenic by a phenylic aromatic moiety; it followed that such model reactions represent well systems with larger aromatic units. Only for the initiation reaction the transition state could not be located; in this case the activation energy was approximated by the change in overall enthalpy.

1. Introduction

Information on the kinetics and thermodynamics of thermal cracking reactions is of great importance for understanding the origin and thermal evolution of oils and natural gases. It is now believed that the thermal evolution of oils is largely controlled by the kinetics of cracking reactions, which occur over geological times (i.e., million years) at temperatures seldom higher than 100 °C.[1] Experimentalists use this hypothesis to simulate the same natural processes, but at much higher temperatures, so most of these cracking reactions proceed sufficiently rapidly to be monitored on an acceptable time scale. Although this approach might be acceptable to elaborate mathematical models that describe oil-cracking processes, it contains some serious shortcomings. Even at high temperatures, the monitoring time can take up to several months. Additionally, the extrapolation from laboratory reactions to geological conditions is not always satisfactory. For example, stoichiometric and kinetic parameters, such as activation energy, frequency factor, and reaction order, can vary significantly upon changing the temperature. Consequently, in cases where the difference in temperature between model and natural circumstances is relatively large, the uncertainty factor in these parameters increases correspondingly. Especially in these cases computational chemistry provides some attractive alternatives to acquire the desired thermodynamic data. Today, quantum mechanical methods, such as those based on density functional theory, offer often amazingly accurate determination of thermodynamic parameters, within a reasonable amount of computer time.[2] This was recently shown for instance, by the calculation of bond dissociation energies of medium-sized aromatic hydrocarbons.[3] Computational approaches offer the possibility to "access" transition state (TS) structures from which, within the approach of transition state theory (TST),[4] valuable information on the kinetics of the reactions can be derived. TST assumes an equilibrium energy distribution among

all possible quantum states at all points along the reaction coordinate, i.e., the lowest energy reaction path from reactants to products via the TS where the energy has its maximum. The probability of finding a molecule in a given quantum state is proportional to the Boltzmann distribution: $\exp(-\Delta E/k_B T)$. If we assume that the molecules at the TS are in equilibrium with the reactant, the macroscopic rate constant (k) can be expressed thermodynamically by an equilibrium constant defined as follows:[5]

$$k = \kappa \left(\frac{p_0}{R'T}\right)^{1-m} (k_B T/h) \exp(-\Delta G^{\ddagger}/RT) \quad (I)$$

In eq I, κ is the transmission coefficient (set to 1 in this study), k_B is Boltzmann's constant, h is Planck's constant, T is the absolute temperature, $R = 8.314\,51$ J·mol·K^{-1}, and $\Delta G^{\ddagger}$ is the gas-phase Gibbs free energy of activation at the reference pressure p_0. In the case of reactions involving two reactants, a reference concentration term remains in eq I, which can be expressed using the ideal gas relationship at a given reference state (m is the number of reactants). For the rate constant k to have dimensions of moles per liter per second, we have assumed a reference pressure of 1 bar with the corresponding perfect gas constant $R' = 0.083\,15$ L·bar·mol^{-1}·K^{-1}.

However, TS structures are often not so easy to locate because there is no general algorithm that successfully leads to a TS on the multidimensional potential energy surface.[6] In fact, a pronounced energy barrier, which corresponds to the TS structure upon going from the reactant to the product, is usually not observed for homolytic dissociation reactions. It is said that in those cases the TS is loose, a case that makes the TS search even more complicated. Yet, we have recently shown that TS structures can be "localized" with the use of canonical or generalized transition-state theory even though these TS structures are rather "loose".[7] Instead of locating the TS on the self-consistent field (SCF) energy surface, it is now located on the Gibbs free energy surface, as shown in Figure 1, which is equivalent to using variational TST[8] instead of conventional

* Corresponding author. Phone: +33 (0)1.47.52.69.10. Fax: +33 (0)1.47.52.70.19. E-mail: francois.lorant@ifp.fr.
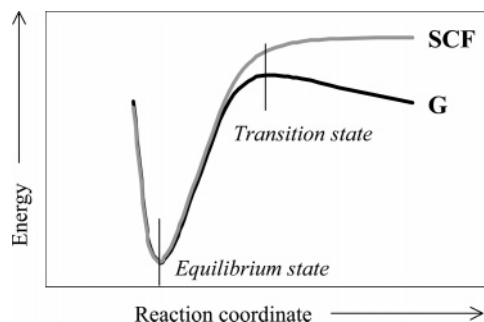† Institute Français du Pétrole.
‡ California Institute of Technology.

Thermal Decomposition of 9-Methylphenanthrene

J. Phys. Chem. A, Vol. 108, No. 46, 2004 **10303**

Figure 1. Comparison between the potential energy surface with (*G*) and without (*SCF*) zero-point, enthalpic and entropic contributions.

TST. Inclusion of the entropy and thermal enthalpy corrections to the SCF energy might not just change the exo-/endoergicity of the reaction but also change the curvature where the TS might be found. We found that application of this approach to the dissociation of ethane into its methyl radicals yielded excellent results in comparison with other theoretical studies and experimental data.[7]
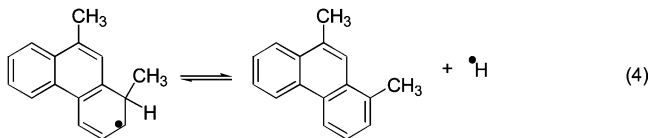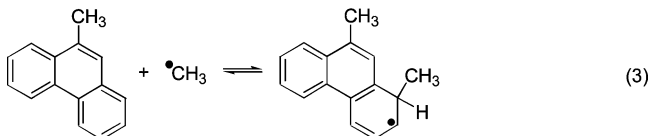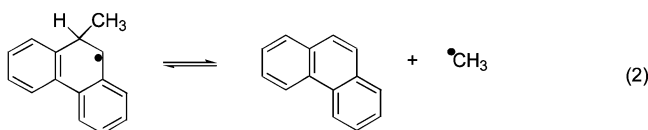
In this paper we present an analogous quantum mechanical study, performed at the uB3LYP/6-31G(d,p) level, on a selected number of elementary reactions (displayed in Scheme 1), which play an important role in the cascade of reaction involved in
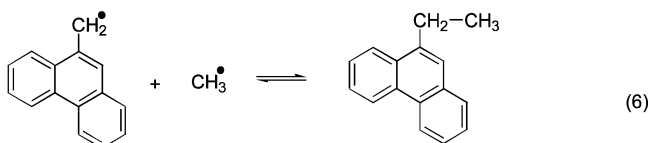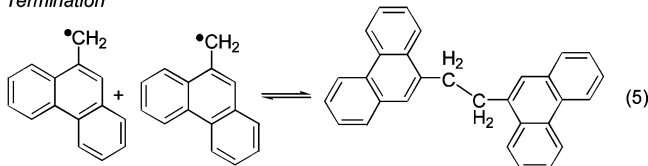
SCHEME 1

Initiation
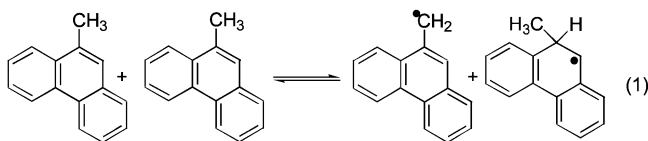
Propagation

Termination

the cracking of 9-methylphenanthrene (9-MPh). The first reaction (reaction 1) is a bimolecular initiation reaction, a reverse radical disproportionation reaction, forming the 9-methylphenanthryl radical and a 9-methylhydrophenanthryl radical. Furthermore, three propagation reactions have been investigated: first, the dissociation of a methyl radical from 9-methylphenanthryl radical (reaction 2); second, the attack of a methyl radical on 9-methylphenanthrene (reaction 3); third, the dissociation of a hydrogen radical from 1,9-dimethylphenanthryl radical, formed during the second propagation, to yield 1,9-dimethylphenanthrene (reaction 4). Two termination or recombination reactions have been studied: the recombination of two 9-methyl-enephenanthrene radicals (reaction 5) and the recombination of a methyl radical with 9-methylenephenanthrene radical (reaction 6). Note that radical hydrogen transfer and abstraction mechanisms were not included in this study, because these reactions are usually very fast compared to other elementary reactions. Therefore, they do not constitute limiting steps in the thermal decomposition scheme of 9-MPh. It should also be added that Scheme 1 is far from complete in describing all reactions that play a role in the cracking of 9-MPh. However, the reactions that are presented are thought to play a significant role and are therefore described quantum mechanically. Our final objective is to build up a much more complete cracking scheme in which a combination of quantum mechanical and empirical calculations will be presented.

9-Methylphenanthrene has been chosen because it represents well the alkylaromatic compounds, which are important intermediates in the oil formation from kerogen. The objective of this work is to locate the TS structures for each of the six reference reactions. Their corresponding activation energies will be used in a later study in which we apply a more empirical model to calculate all reactions thought to play a role in the complete cracking scheme of 9-MPh. As in ref 7, we will increase the length of the bond that is to be cracked in a stepwise manner. At each step, the structure is optimized, keeping only the length of the bond under investigation constant. In those cases where the energy profile already shows a maximum upon homolytic bond breaking at 0 K, a complete (i.e., without constraints) optimization of the transition state structure is performed.

2. Theoretical Methods

The majority of the geometry optimization calculations were performed with the Jaguar suite of programs,[9] at the unrestricted B3LYP/6-31G(d,p) level and making use of the pseudospectral method. Only in those cases where the reference reaction was replaced by a model system (vide infra) was the Gaussian 98 (G98) package of programs[10] used for the geometry optimization. It appeared to be very important to check the energy of the wave function, especially for the "small" model compounds. It was found that the total energy did not always converge to the bond dissociation energy upon stepwise increase of the bond to be homolytically broken. Independent of how the converged wave function was obtained, either by a default guess or by superposition of another wave function coming from a slightly different optimized geometry, it appeared crucial to check the wave function stability. With use of the G98 stable=opt keyword, the stability was checked after the first SCF cycle. However, it was noticed that, especially at larger (>2.5 Å) bond-breaking distances, the stable wave function could become significantly spin contaminated with values of S^2 up to 1.04.

Next, the geometry was optimized with its stable wave function, and finally, after completion of the geometry optimiza-
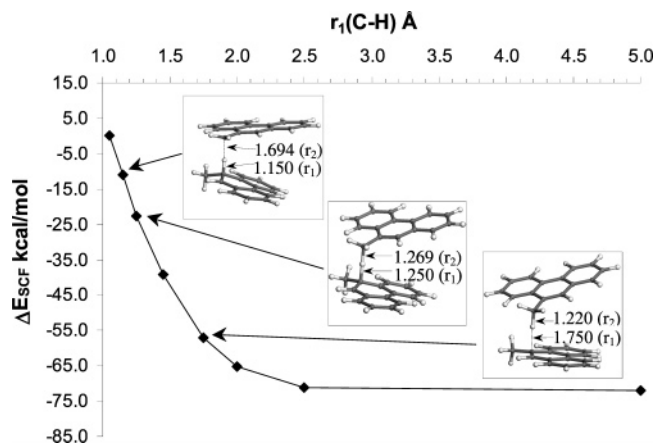
Figure 2. Change in energy (kcal/mol) with respect to the structure in which $r_1 = 1.050$ Å, and the distance $r_2(C-H)$ (Å) as a function of r_1 in reaction 1.

Figure 3. Gibbs free energy as a function of $r(C-H)$ at different temperatures for the dissociation of a hydrogen radical from toluene. The energy of the structure in which $r(C-H)_{eq}$ is the equilibrium distance has been taken as a reference.

tion, the wave function was again subjected to a stability analysis. With this approach the total energy converged nicely to the dissociation energy upon increasing the bond length of the bond to be cracked.[11] Yet, for the recombination reactions (5 and 6) it was important to treat the two reactants in two different systems when the distance between them was larger than 3.5 Å.

All structures were optimized, either without any constraints (reactants, products, and transition state structures that could be directly located on the SCF potential energy surface), or upon freezing the bond length corresponding to the reaction coordinate, which was increased in a stepwise manner to represent the dissociation process. All final optimized geometries were subjected to a frequency analysis performed at the same level of theory as the geometry optimization. For the evaluation of the vibrational modes the standard methods in the G98 program have been applied without any additional procedures. Furthermore, there has been no scaling factor used for the frequencies, which are in their turn used to calculate the thermodynamic properties G, H, and S. In addition, no corrections to the anharmonicities have been applied for the vibrational energies.

CASSCF calculations were realized at the 6-31G(d,p) level with four electrons in the active space consisting of in total four orbitals.

3. Results and Discussion

3.1. Initiation Reaction. The thermal cracking of 9-MPhe is thought be started as a bimolecular reaction in which a hydrogen radical is transferred from one 9-MPhe to another:[12,23]
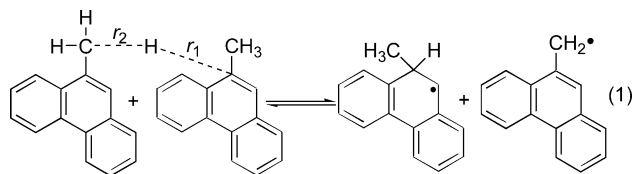
This process, a reverse radical dismutation (RRD), was first evidenced on the anthracenic system.[13] It has been suspected that such an RRD reaction has no energy barrier; however, the energetic of the mechanism has never been explored precisely.[14] Hence, to address this reaction computationally, we started to increase the $r_1(C-H)$ distance in a stepwise manner. Figure 2 shows a part of the potential energy surface (0 K and no zero
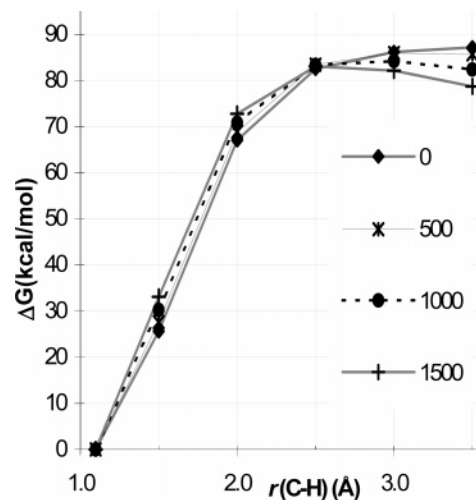
point energy (ZPE) corrections) as function of the distance r_1-(C−H). From this figure it follows that the system's energy is dropping rapidly: from $r_1(C-H) = 1.05$ Å to $r_1(C-H) = 5.0$ Å the system gained almost 70 kcal/mol, in a continuous way, i.e., without any indication of a barrier.

In the same figure it can be seen that a second important carbon−hydrogen bond [$r_2(C-H)$] quickly relaxes to its equilibrium distance, $r_2(C-H)_{eq} = 1.099$ Å. For example, at $r_1(C-H)_{eq} = 1.750$ Å, the r_2 distance has decreased to 1.220 Å.

The ΔSCF curve does not indicate the presence of a transition state structure for this reaction. Although the calculation of the quantum mechanical Hessian matrix is rather weighty for such systems, we have tried to calculate the Gibbs free energy contributions for a few geometries. However, due to the presence of several imaginary frequencies, which proves that we did not locate the TS, the evaluation of the thermodynamic properties contains significant errors.

Alternatively, we investigated the same reaction in a non-concerted way, i.e., the homolytic dissociation of a hydrogen radical from the methyl group, which subsequently attacks the aromatic ring of another 9-MPh. Since we do not expect a significant influence of the aromatic moiety on the bond dissociation energy of a hydrogen radical from the methyl group,[15] the first step of the reaction was modeled by the dissociation of a hydrogen radical from the methyl group of toluene; see Figure 3. This figure nicely shows the entropic effects with increasing temperature on the change in the Gibbs free energy (ΔG). It can be seen that upon increasing the distance $r(C-H)$ the system becomes less stable as compared to the structure of toluene with $r(C-H)_{eq}$, which is taken as a reference. At low temperatures (0 K) this curve does not show any maximum. However, upon increase of the temperature it can be seen that, e.g., at 1500 K, a maximum starts to appear around 2.5 Å. Further increase of the temperature pronounces more the maximum of the potential energy, which additionally slightly shifts toward $r(C-H)_{eq}$. We have calculated a bond dissociation enthalpy (BDE) of ΔH(300 K) = 86.8 kcal/mol, which approaches the literature value of 89.7 kcal/mol.

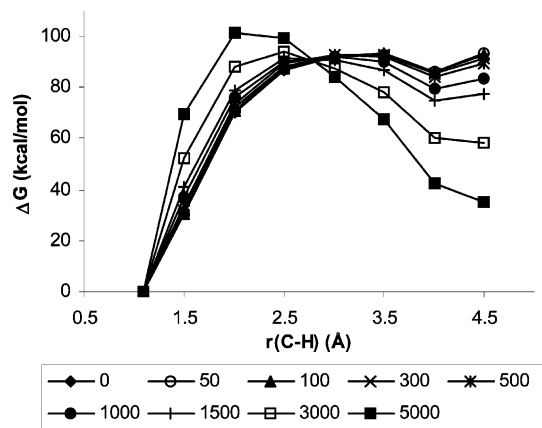To overcome the problems of spin contamination with the uB3LYP method (see Theoretical Methods) and small imaginary

Thermal Decomposition of 9-Methylphenanthrene

J. Phys. Chem. A, Vol. 108, No. 46, 2004 **10305**

Figure 4. Change in the Gibbs free energy as function of the $r(C-H)$ distance at different temperatures (K) calculated with CASSCF(4,4)/6-31G(d,p) level.

frequencies that were calculated with increasing $r(C-H)$ distance in the dissociation reaction of the hydrogen radical from the methyl group of toluene, the calculation was also performed with the multireference CASSCF method;[16] see Figure 4. With this method wave functions are obtained that do not suffer from spin contamination. Furthermore, even at distances $r(C-H) > 3.5$ Å, there is only one imaginary frequency, corresponding to the reaction coordinate, which nicely goes to zero upon further increase of the $r(C-H)$ distances. However, the calculated BDE does not approximate as well as the B3LYP functional the experimental BDE value: $\Delta H(300 \text{ K}) = 97.0$ (CASSCF), 86.9 (B3LYP), and 89.7 kcal/mol (experimentally).[17] This larger difference might be caused by the too small 6-31G(d,p) basis set. Indeed, more electrons and orbitals in the active space would give a better description. Yet, such CASSCF calculations would already become very intense for the toluene system and prohibitive for the larger molecular systems such as 9-MPh. Consequently, we continued to use the initial B3LYP/6-31G-(d,p) approach.

It was calculated that the bond dissociation energy for the formation of a hydrogen radical is on the order of 10 kcal/mol higher, as compared to the change in the Gibbs free energy for

the concerted reaction in which the phenanthrene part was replaced by a phenyl ring. This suggests that of the two compared initiation reactions the concerted reaction would be the preferred one (at low temperatures). Likewise, the concerted reaction will probably be also the preferred reaction for the phenanthrene system (reaction 1).

Since we could not locate a transition state for reaction 1, we have calculated $\Delta H(300 \text{ K}) = 58.3$ kcal/mol, following therefore the conclusions of previous authors,[18] and we assume that the activation energy E is close to this value.

3.2. Propagation Reactions. The first propagation reaction (2) creates a methyl radical. Figure 5 shows the Gibbs free

(2)
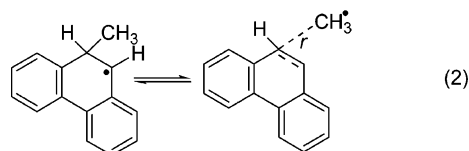
energy as function of the distance $r(C-C)$ at different temperatures. In contrast to reaction 1, it can be seen that already at 0 K (without inclusion of zero-point energies), the energy profile shows a maximum (at 2.292 Å). This transition state structure is 24.2 kcal/mol less stable than the reference structure with $r(C-C)_{eq}$. Increase of the temperature up to 1500 K shows that the reaction becomes relatively more exothermic. The dissociation of the methyl radical is an endoergic reaction at low temperatures ($T < 500$ K), but becomes exoergic at 1000 K and above. This is of course a result of entropy, which has larger contributions as the methyl group dissociates.

The energy maximum (the TS structure) shifts from 2.29 to 2.2 Å and this structure becomes relatively more stable: 21.5 kcal/mol with respect to the energy of the TS at 0 K, as shown in Table 1.

It can be argued that by applying exclusively the harmonic oscillator model, which is used by default in G98 to evaluate the vibrational modes, serious errors are introduced especially for those structures that resemble the TS structure. As the methyl radical is dissociating from the aromatic phenanthrene moiety, a partition function that corrects for the hindered rotation should be used, and finally the partition function for a free rotor. To
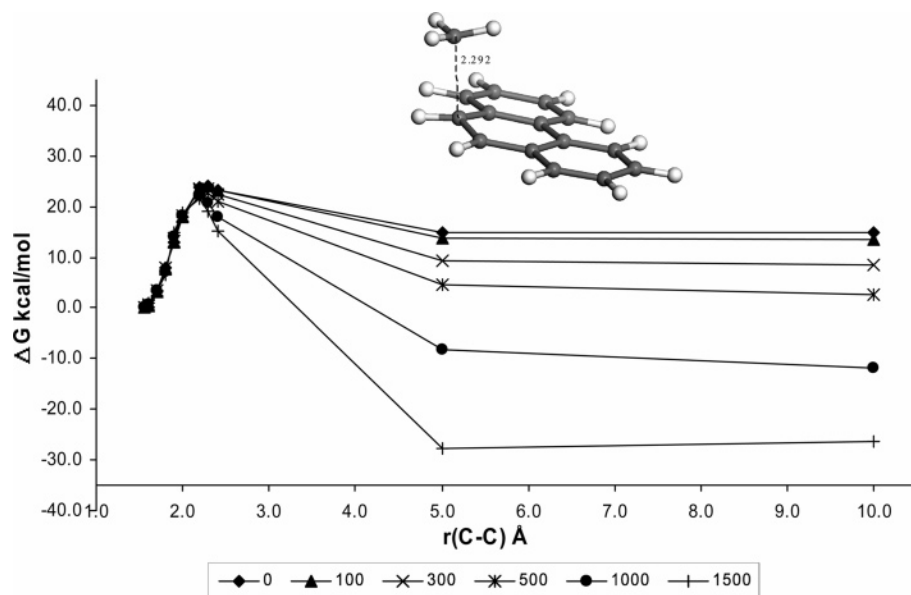

Figure 5. Change in Gibbs free energy for reaction 2 as a function of the distance $r(C-C)$ at different temperatures with respect to the structure in which $r(C-C)$ is the equilibrium distance.

TABLE 1: Relative Stabilities (Changes in Gibbs Free Energies, ΔG (kcal/mol)) with Respect to the Distance $r(C-C)_{eq}$ and Contribution from the Hindered Methyl Rotation (ω) for Structures Close to the TS Structures at Different Temperatures for Reaction 2

| temp (K) | $r(C-C)$ (Å) | | | | | |
| | 2.0 | | 2.2 | | 2.290 | |
	ΔG	ω	ΔG	ω	ΔG	ω
0	18.0		23.8		24.2[a]	
50	18.0	0.00	23.9	0.00	24.1	0.00
100	18.0	0.00	23.9	0.00	24.1	0.00
300	18.3	0.03	23.6	0.05	23.6	0.10
500	18.1	0.12	23.3	0.18	22.8	0.29
1000	18.3	0.56	22.3	0.73	20.8	1.04
1500	18.8	1.21	21.5	1.52	19.1	2.03

[a] Numbers in italics represent the maximum values for the curves in Figure 5.

do so, we have applied the interpolating function suggested by Truhlar.[19] We first analyzed the (harmonic) vibrational modes for all the calculated structures of reaction 2. Figure 6 shows the six vibrational modes with wavenumbers that go to 0 cm^{-1} upon increase of the $r(C-C)$ bond; e.g., the curve with the dotted line and solid squares corresponds to the reaction coordinate. The other modes displayed with dotted lines become the other two transitional modes of the outgoing methyl group. The three modes with the solid lines belong to the three rotational modes of the dissociating methyl group. With the interpolating function of Truhlar we have calculated corrections for the hindered rotation (ω) around the z-axis on the order of 1.5−2.0 kcal/mol for the structures in the region where the TS structure is located. These corrections are relatively small with respect to the overall error made at this level of theory [uB3LYP/6-31G(d,p)], which is estimated to be around 5−6 kcal/mol.[3] Therefore, we will neglect in our other calculations the error due to the hindered rotation and free rotor.

Reaction 3 is very similar to reaction 2 in that there is also a methyl radical involved:
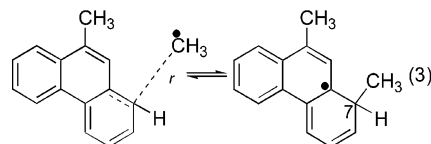
Figure 7 shows that the attack of this methyl radical on the 1-position is an exoergic reaction, which becomes only slightly endoergic at very high temperatures (1500 K): 1.1 kcal/mol.[20] As for reaction 2 upon increase of the temperature (0 → 1500 K), the maxima of the curves shift to slightly smaller $r(C-C)$ distances, whereas the height of the barrier is slightly less affected (Table 2): $\delta\Delta G = 1.9$ kcal/mol compared to 2.7 kcal/mol for reaction 2.

The third propagation reaction that was investigated is the formation of a hydrogen radical out of the 1,9-dimethylphenanthrene radical, "created" by reaction 3:
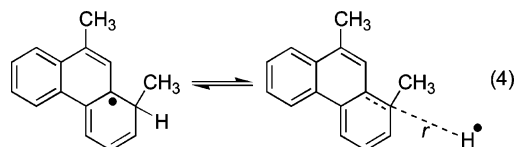
As there is only a hydrogen radical that dissociates, the entropic contributions are thought to be relatively small, and it is seen in Figure 8 that for this reaction the energy profile is almost entirely determined by the enthalpic term.[20] Consequently, the maxima of the energy profile hardly change neither in height nor in position, 1.9 kcal/mol and 0.093 Å, respectively (Table 3).
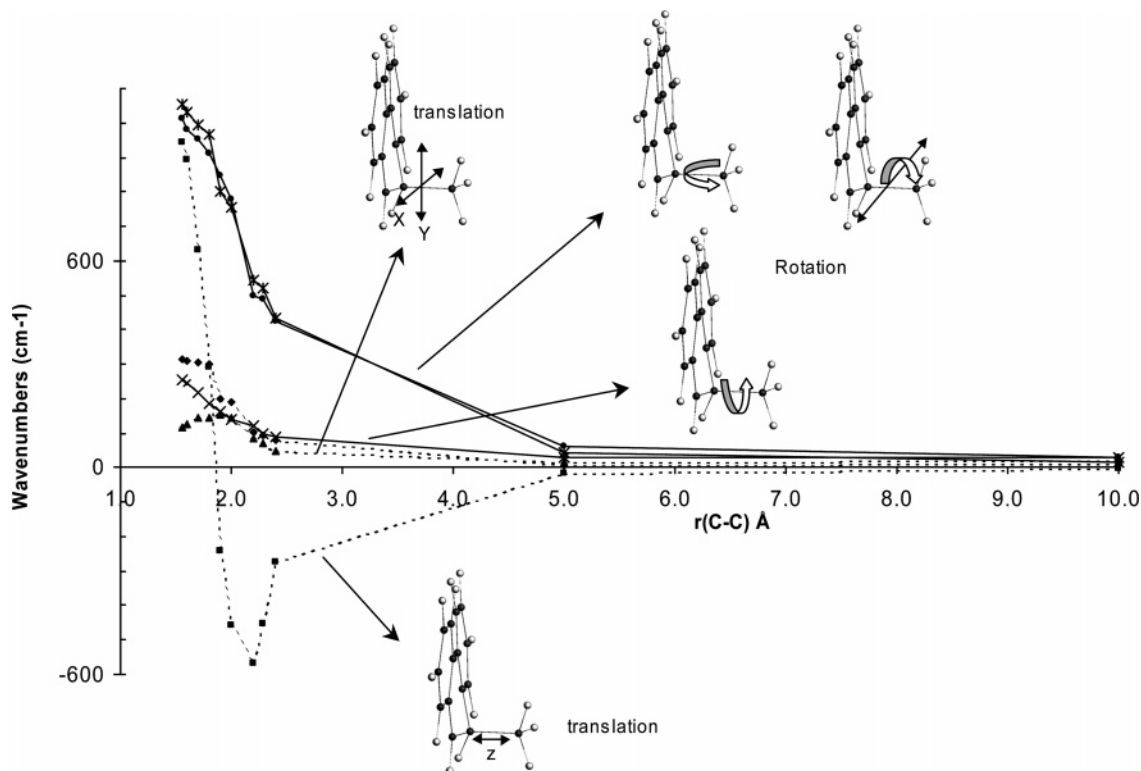

Figure 6. Selected normal vibrational modes of reaction 2. The graphs with dotted lines represent the vibrational modes that become translational modes, of which the graph with the solid squares represents the reaction coordinate; the graphs with solid lines represent the vibrational modes that become rotational modes upon increasing distance.

Thermal Decomposition of 9-Methylphenanthrene

J. Phys. Chem. A, Vol. 108, No. 46, 2004 **10307**

TABLE 2: Relative Stabilities (Changes in Gibbs Free Energies, ΔG (kcal/mol)) with Respect to the Distance $r(C-C)_{eq}$ and Contribution from the Hindered Methyl Rotation (ω) for Structures Close to the TS Structures at Different Temperatures for Reaction 3

| | $r(C-C)$ (Å) | | | | | |
| | 2.1 | | 2.266 | | 2.3 | |
temp (K)	ΔG	ω	ΔG	ω	ΔG	ω
0	21.4		23.2[a]		23.0	
50	21.4	0.00	23.2	0.00	23.0	0.00
100	21.4	0.00	23.2	0.00	23.0	0.00
300	21.4	0.03	22.7	0.05	22.4	0.05
500	21.3	0.12	22.2	0.16	21.7	0.18
1000	21.2	0.55	20.6	0.67	19.7	0.74
1500	21.3	1.20	19.3	1.40	18.0	1.53

[a] Numbers in italics represent the maximum values for the curves in Figure 7.

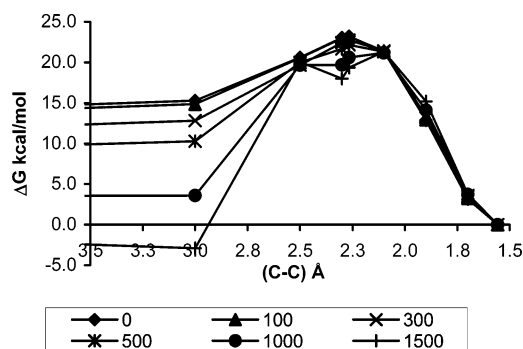**Figure 7.** Change in Gibbs free energy for reaction 3 as a function of the distance $r(C-C)$ at different temperatures with respect to the structure in which $r(C-C)$ is the equilibrium distance.
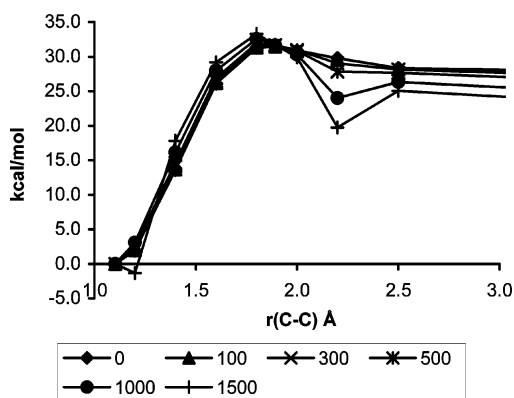

Figure 8. Change in Gibbs free energy for reaction 4 as a function of the distance $r(C-H)$ at different temperatures. The energy of the structure in which $r(C-H)$ is the equilibrium distance has been taken as a reference.

3.3. Termination Reactions. Two termination reactions have been investigated: the recombination of two 9-methylphenanthrene radicals, and the recombination of a methyl radical with a 9-methylphenanthrene radical. We will first discuss the former recombination reaction:
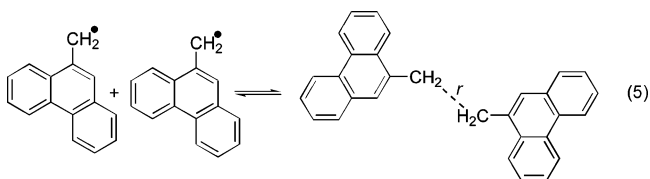

TABLE 3: Relative Stabilities (Changes in Gibbs Free Energies (kcal/mol)) with Respect to the Distance $r(C-C)_{eq}$ for Structures Close to the TS Structures at Different Temperatures for Reaction 4

| | $r(C-H)$ (Å) | | |
temp (K)	1.6	1.8	1.893
0	26.1	31.3	31.4[a]
50	26.1	31.3	31.4
100	26.1	31.3	31.5
300	26.5	31.6	31.6
500	26.9	31.9	31.7
1000	28.0	32.6	31.6
1500	29.2	33.3	31.7

[a] Numbers in italics represent the maximum values for the curves in Figure 8.

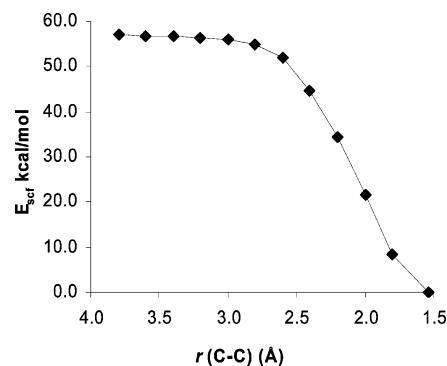**Figure 9.** Change in SCF energy as a function of the $r(C-C)$ distance with respect to structure with $r(C-C)_{eq}$ for reaction 5.

Note that these geometry optimizations were performed in C_i symmetry. Figure 9 shows the profile of the SCF energy upon decrease of the $C-C$ bond. It can be seen that the homolytic bond dissociation costs about 57 kcal/mol. The E_{scf} curve (0 K without ZPE corrections) does not show any barrier for the creation of the two radicals (reaction 5 in the opposite direction). As expected, this dissociation reaction is again largely determined by enthalpic contributions. Since inclusion of the Gibbs free energy corrections on these systems (560 basis functions with the 6-31G(d,p) basis set) is computationally very demanding, we have chosen to replace the phenanthrene moiety by the much smaller phenyl one as we did for the initialization reaction. We are aware that the size of the aromatic part will influence the bond strength of the $C-C$ bond. Analysis of the "full" reaction would enormously increase the total computational time (with respect to the phenyl system), making the computational approach a less attractive alternative with respect to a traditional laboratory experiment.

Upon replacement of the aromatic phenanthrene system by a phenyl one, the reaction simplifies to the recombination of two benzyl radicals to give 1,2-diphenylethane:
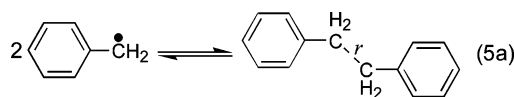
In Figure 10 the changes in the Gibbs free energy at different temperatures are displayed, and it can be seen that at low temperatures ($T < 1000$ K) the ΔG curves do not show any barrier. The barrier starts to appear at 1000 K and becomes very pronounced at 3000 K. Consequently, it is necessary to go to very high temperatures to show an activation barrier for the creation of two radicals.
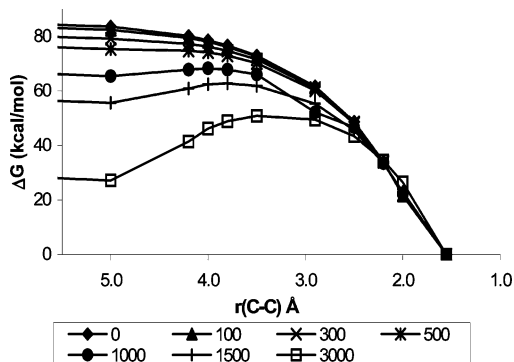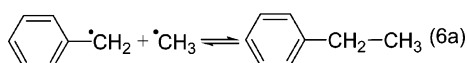
Figure 10. Change in Gibbs free energy with respect to 1,2-diphenylethane (reaction 5a) at different temperatures.

The second termination reaction was simplified as well and was modeled by the recombination reaction of a methyl and benzyl radical:

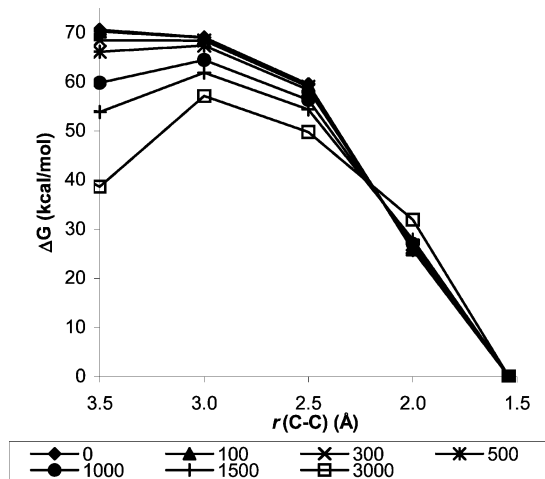The corresponding changes in Gibbs free energy curves are shown in Figure 11.[21]

Figure 11. Change in Gibbs free energy with respect to phenylethane (reaction 6a) at different temperatures.

3.4. Rate Constant (k), Activation Energy (E), and Prefactor (A). The rate constant can be calculated with the use of eq I. Upon plotting $\ln(k/T)$ vs $1/T$, the activation enthalpy and entropy can be calculated from the slope ($\Delta H^{\ddagger}/RT$) and intercept ($\ln(k_B/T + \Delta S^{\ddagger}/R)$). To compare the activation energy and prefactor from quantum mechanical calculations that use fixed temperature and pressure with the experimental ones (expressed in concentrations), eqs II and III were applied:

$$E = \Delta H^{\ddagger} + (1 - \Delta n)RT \qquad \text{(II)}$$

$$\ln A = \ln\left(\frac{k_B T}{h}\right) + \frac{\Delta S^{\ddagger}}{R} - \Delta n \ln(R'T) + (1 - \Delta n) \quad \text{(III)}$$

$$A = \left(\frac{k_B T}{h}\right) \exp\left(\frac{\Delta S^{\ddagger}}{R}\right)(R'T)^{-\Delta n} \exp(1 - \Delta n) \qquad \text{(IV)}$$

In these equations Δn is the change in moles ($\Delta n = 0$ for unimolecular reactions and $\Delta n = -1$ for association or recombination reactions, $R' = 0.082\,057\,8$ dm^3·atm·K^{-1}·mol^{-1}).[22] Dissociation reactions are considered to be unimolecular, since
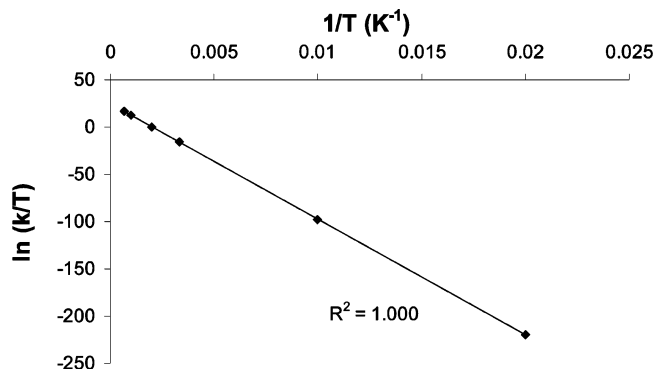

Figure 12. Correlation between k/T and $1/T$ for reaction 2.

there is no change in moles going from reactant to activated species, whereas the reversed dismutation, addition, and recombination reactions are taken as bimolecular reactions.

In general, plotting $\ln(k/T)$ vs $1/T$ yields a very good correlation as can be seen for example in Figure 12 for the dissociation of a methyl radical, reaction 2.

The correlation for the two recombination reactions 5a and 6a is somewhat less linear as can be seen from the correlation factor R. Moreover, these reactions also show a positive slope as can be seen in Figure 13. Such positive slopes might indicate that the rate of recombination of radicals to form closed-shell species is higher for fragments with low internal energy; as the temperature increases this population reduces, and consequently the effective rate of recombination decreases.

Table 4 and Figure 14 summarize the calculated activation energies (E) and preexponential frequency factors (A) for the investigated reactions (1−6). The results are compared with their analogous reactions of 1-methylpyrene[23] (reactions 1−4) and reactions 5 and 6 with the same reaction.

The approximated activation energy for reaction 1 differs significantly from the value reported by Smith and Savage.[23] In their publication they have taken the activation energy for this reaction equal to the heat of reaction, since they assume that the reverse reaction, i.e., the radical disproportionation reaction, is almost zero. Hence, they calculated for the reverse radical disproportionation reaction $\Delta H = 45.8$ kcal/mol [the sum of the reaction methylpyrene → methylpyrenyl radical + H$^{\bullet}$ ($\Delta H = 82.9$)[24] and the reaction pyrene + H$^{\bullet}$ → 1-hydropyrenyl radical ($\Delta H = -37$ kcal/mol)[25]]. From calculations at the same uB3LYP/6-31G(d,p) level we find an overall value of $\Delta H = 51.9$ kcal/mol, which is expected to be accurate to $\sim$3 kcal/mol. This is consistent with the semitheoretical/experimental value of 45.8 kcal/mol. Furthermore, the $\delta\Delta H$ between the B3LYP values of pyrene (51.9) and 9-MPh (58.3) may be rationalized in terms of the difference in size of the aromatic moiety: the larger pyrene aromatic unit will increase the stabilization for creating the two radicals as compared to the phenanthrene unit.

The approximate value of ΔH for the reverse radical disproportionation reaction gives a plausible result. However, without a transition state we cannot estimate the prefactor A. Currently we are investigating different methods to reexamine this reaction.

For the propagation reactions, good to excellent agreement was obtained with respect to experimental data. Only the activation energy of the methyl addition reaction 3 is likely to be overestimated by our calculations: 9.4 kcal/mol, whereas experimental data show only 4.1 kcal/mol. On the other hand, its inverse reaction, i.e., the dissociation reaction, is in much
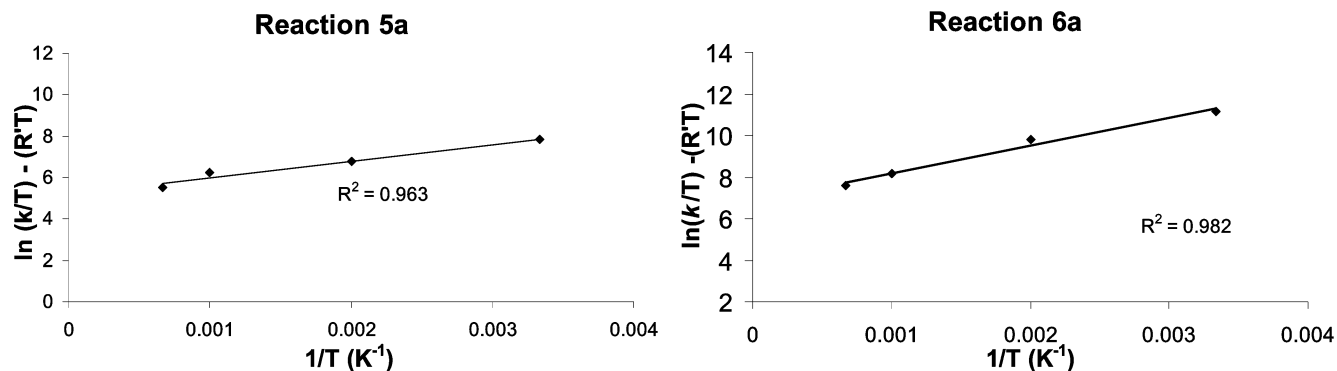
Thermal Decomposition of 9-Methylphenanthrene

J. Phys. Chem. A, Vol. 108, No. 46, 2004 **10309**

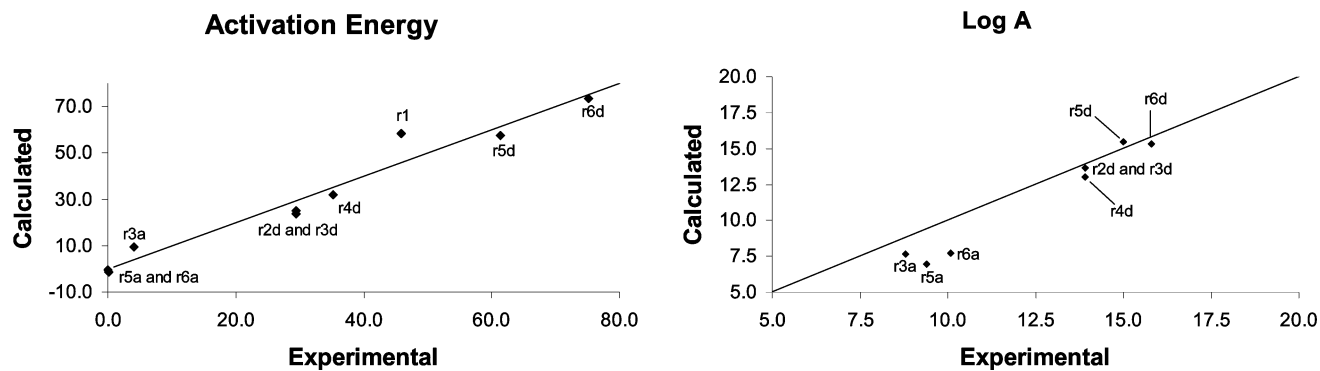**Figure 13.** Positive slope for the recombination reactions 5a (left) and 6a (right).

Figure 14. Correlation between calculated and experimental data (a, association; d, dissociation).

TABLE 4: Calculated E and A (at 300 K) for the Six Reference Reactions Compared to Experimental Data in Parentheses

	reaction 1	reaction 2	reaction 3	reaction 4	reaction 5 (diphenylethane)	reaction 6 (ethylbenzene)
E (kcal/mol)	58.3[a] (45.8)[b]	24.9 (29.4)[b]	9.4 (4.1)[b]	32.0 (35.3)[b,c]	−0.4 (0)[e]	−1.5 (0.2)[d]
log A (s⁻¹ or L·mol⁻¹·s⁻¹)		13.7 (13.9)[b]	7.6 (8.8)[b]	13.0 (13.9)[b,c]	7.0 (9.4)[e]	7.7 (10.1)[d]

[a] ΔH(300 K) value. [b] Evaluated data from the analogous reaction with 1-methylpyrene:[23]
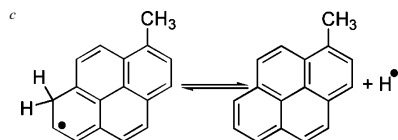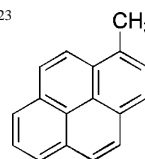
[d] Reference 31. [e] Reference 29.

better agreement with the experimental data: 23.9 (calculated) with respect to 29.4 (experimentally).[23]

For reaction 5, both the recombination and dissociation reactions, the calculated activation energy and the prefactor for reaction also are in harmony with experimental data.[26] For the dissociation reaction at 713 K we have calculated $E = 57.7$ kcal/mol (literature 61.4) and log $A = 15.4$ (literature 15.0).[27,28] The calculated rate constant also agrees reasonably well with the experimental data, k(713 K) $= 1.43 \times 10^{-4}$ (experimentally) with respect to 5.61×10^{-3} s⁻¹ (calculated). For the recombination reaction we calculated at 500 K $E = 0.4$ kcal/mol and log $A = 7.4$ L·mol⁻¹·s⁻¹ as compared to the experimental values of 0.0 kcal/mol and 9.4 L·mol⁻¹·s⁻¹.[29] Due to underestimation of the prefactor, our calculated specific rate constants are also underestimated with respect to the experimental ones, for example, k(500 K) $= 3.01 \times 10^9$ (experimentally)[29] as compared to 4.02×10^7 L·mol⁻¹·s⁻¹ (calculated).

For the second termination reaction, reaction 6, we have calculated for the dissociation reaction at 1000 K an activation energy of $E = 73.3$ kcal/mol and prefactor of log $A = 15.3$ s⁻¹, which corresponds well to the experimental values: $E = 75.1$ kcal/mol and log $A = 15.8$ s⁻¹. Furthermore, the specific rate k(1000 K) is calculated to be 1.99×10^{-1}, as compared to the experimental 2.34×10^{-1} L·mol⁻¹·s⁻¹.[30] For the recombination reaction the activation corresponds well to the experimental value $E = -1.5$ and 0.2 kcal/mol, respectively. The prefactor, and consequently the specific rate constant, is again underestimated by our calculations: log $A = 7.7$ L·mol⁻¹·s⁻¹ and k(300 K) $= 6.0 \times 10^8$ L·mol⁻¹·s⁻¹ as compared to the experimental values of 10.1 L·mol⁻¹·s⁻¹ and 8.22×10^9 L·mol⁻¹·s⁻¹.[31]

From these data it can be concluded that dissociation reactions are well described by our calculations as are the activation energies of the bimolecular reactions, suggesting that the uB3LYP functional in combination with the 6-31G(d,p) basis set provides a "solid" level of theory. Yet, for the bimolecular (5 and 6) reactions the specific rate constants are somewhat underestimated.

4. Conclusions

In this density functional study we have investigated six representative radical reactions that plausibly play an important role in the cracking process of 9-methylphenanthrene. At the uB3LYP/6-31G(d,p) level we located for the three propagation reactions the transition structures at the potential energy surface at 0 K. The corresponding calculated activation energies are in good agreement with experimental data. The transition states for the two termination reactions could not be determined directly; i.e., for these reactions the phenanthrenic aromatic moiety needed to be reduced to a phenylic group due to large computational times. It was shown that the inclusion of the entropy in combination with high temperatures can significantly change the endo-/exothermicity of the reactions. More importantly, the loose transition states for the forward and reverse (dissociation) reactions were considerably tightened by application of this approach. From the calculations with uB3LYP functional it follows that our model systems present good alternatives for the real 9-MPhe system, and a fine accord with the literature values was obtained for all dissociation reactions that were investigated. The calculated activation energies for the studied bimolecular reactions generally correspond well to their experimental values, yet the prefactors are somewhat underestimated by the method used.

For the initiation reaction the transition state could not be located, neither by inclusion of entropy nor by simplifications of the aromatic moiety. It is even doubtful whether this reaction has (intrinsically) a transition state, and as an approximation, the ΔH was used to approximate the activation energy.

Although the final wave functions obtained for the initiation and termination reactions suffer from spin contamination, the overall B3LYP results are in better agreement with experimental data than those of, e.g., the CASSCF method. It should, however, be noted that this latter type of calculation is in principle the better method for describing homolytic dissociation reactions. Yet, to reach experimental or thermodynamic accuracy, it seems that a larger active space is needed in combination with a larger basis set than the 6-31G(d,p), which make these calculations on substituted 9-MPhe molecules for the moment prohibitive.

Generally, it can be concluded that the chosen level of theory [uB3LYP/6-31G(d,p)] yields results that are in good agreement with experimental values in a reasonable amount of time. However, an improvement of the method is necessary to reproduce more accurately the experimental prefactors for the initiation and recombination reactions.

References and Notes

(1) Tissot, B. P.; Welte, D. H. *Petroleum Formation and Occurrence*, 2nd ed.; Springer-Verlag: Berlin, 1994.

(2) (a) Chandra, A. K.; Uchimaru, T. *J. Phys. Chem. A* **2000**, *104*, 9244−9249. (b) Saeys, M.; Reyniers, M.-F.; Marin, G. B.; Van Speybroeck, V.; Waroquier, M. *J. Phys. Chem. A* **2003**, *107*, 9147−9159. (c) Van Speybroeck, V.; Reyniers, M. F.; Marin, G. B.; Waroquier, M. *Chemphyschem* **2002**, *3*, 863−870.

(3) Yao, X.-Q.; Hou, X.-J.; Wu, G.-S.; Xu, Y.-Y.; Xiang, H.-W.; Jiao, H.; Li, Y.-W. *J. Phys. Chem. A* **2002** *106*, 7184−7189.

(4) (a) Eyring, H. *J. Chem. Phys.* **1935**, *3*, 107. (b) Glasstone, S.; Wynne-Jones, W. F. L.; Eyring, H. *J. Chem. Phys.* **1935**, *3*, 492. (c) Laidler, K. J.; Eyring, H. *The Theory of Rate Processes*; McGraw-Hill: New York, 1941.

(5) Benson, S. W. *Thermochemical Kinetics*, 2nd ed.; J. Wiley & Sons: New York, 1976.

(6) Several methods are described in: Jensen, F. *Introduction to Computational Chemistry*; Wiley: Chichester, 1999; pp 327−338.

(7) Lorant, F.; Behar, F.; Goddard, W. A., III; Tang, Y. *J. Phys. Chem. A* **2001**, *105*, 7896−7904.

(8) Issacson, A. D.; Truhlar, D. G. *J. Chem. Phys.* **1982**, *76*, 1380.

(9) *Jaguar 4.1*; Schrodinger, Inc.: Portland, OR, 1991−2000.

(10) Frisch, M. J.; Trucks, G. W.; Schlegel, H. B.; Scuseria, G. E.; Robb, M. A.; Cheeseman, J. R.; Zakrzewski, V. G.; Montgomery, J. A., Jr.; Stratmann, R. E.; Burant, J. C.; Dapprich, S.; Millam, J. M.; Daniels, A. D.; Kudin, K. N.; Strain, M. C.; Farkas, O.; Tomasi, J.; Barone, V.; Cossi, M.; Cammi, R.; Mennucci, B.; Pomelli, C.; Adamo, C.; Clifford, S.; Ochterski, J.; Petersson, G. A.; Ayala, P. Y.; Cui, Q.; Morokuma, K.; Malick, D. K.; Rabuck, A. D.; Raghavachari, K.; Foresman, J. B.; Cioslowski, J.; Ortiz, J. V.; Baboul, A. G.; Stefanov, B. B.; Liu, G.; Liashenko, A.; Piskorz, P.; Komaromi, I.; Gomperts, R.; R. Martin, R. L.; Fox, D. J.; Keith, T.; Al-Laham, M. A.; Peng, C. Y.; Nanayakkara, A.; Gonzalez, C.; Challacombe, M.; Gill, P. M. W.; Johnson, B.; Chen, W.; Wong, M. W.; Andres, J. L.; Gonzalez, C.; Head-Gordon, M.; Replogle, E. S.; Pople, J. A. *Gaussian 98*, revision A7; Gaussian, Inc.: Pittsburgh, PA, 1998.

(11) As a consequence of the reoptimization of the wave function using stable=opt, the new wave function often becomes rather spin contaminated.

(12) Behar, F.; Budzinski, H.; Vandenbroucke, M.; Tang, Y. *Energy Fuels* **1999**, *13*, 471−481.

(13) Billmers, R.; Griffith, L. L.; Stein, S. E. *J. Phys. Chem.* **1986**, *90*, 517−523.

(14) During the submission process two computational studies have been published that show the existence of a TS for the disproportionation reaction of $CH_4 + CH_2CH_2 = CH_3^{\bullet} + CH_3CH_2^{\bullet}$: (a) Mousavipour, S. H.; Homayoon, Z. *J. Phys. Chem. A* **2003**, *107*, 8566−8574. (b) Zhu, R. S.; Xu, Z. F.; Lin, M. C. *J. Chem. Phys.* **2004**, *120*, 6566−6573.

(15) In fact, this dissociation reaction energy has been calculated for both systems: $\Delta_f H°$(298 K) = 86.9 and 86.3 kcal/mol for toluene and 9-MPhe, respectively.

(16) (a) Hegarty, D.; Robb, M. A. *Mol. Phys.* **1979**, *38*, 1795−1812. (b) Eade, R. H. E.; Robb, M. A. *Chem. Phys. Lett.* **1981**, *83*, 362−368. (c) Schlegel, H. B.; Robb, M. A. *Chem. Phys. Lett.* **1982**, *93*, 43−46. (d) Bernardi, F.; Bottini, A.; McDougall, J. J. W.; Robb, M. A.; Schlegel, H. B. *Faraday Symp. Chem. Soc.* **1984**, *19*, 137−147. (e) Yamamoto, N.; Vreven, T.; Robb, M. A.; Frisch, M. J.; Schlegel, H. B. *Chem. Phys. Lett.* **1996**, *250*, 373−378. (f) Frisch, M. J.; Ragazos, I. N.; Robb, M. A.; Schlegel, H. B. *Chem. Phys. Lett.* **1992**, *189*, 524−528.

(17) $\Delta_f H°_{gas}$(toluene) = 11.95 ± 0.15 kcal/mol [Prosen, E. J.; Gilmont, R. *J. Res. Natl. Bur. Stand. (U.S.)* **1945**, *34*, 65−70], $\Delta_f H°_{gas}$(benzyl) = 49.5 ± 1 kcal/mol [Tsang, W. Heats of Formation of Organic Free Radicals by Kinetic Methods. In *Energetics of Organic Free Radicals*; Martinho Simoes, J. A., Greenberg, A., Liebman, J. F., Eds.; Blackie Academic and Professional: London, 1996; pp 22−58], and $\Delta_f H°_{gas}$(H$^{\bullet}$) = 52.103 ± 0.001 kcal/mol [Cox, J. D.; Wagman, D. D.; Medvedev, V. A. *CODATA Key Values for Thermodynamics*; Hemisphere Publishing Corp.: New York, 1984; p 1]. BDE = 52.103 + 49.5 − 11.95 = 89.7 kcal/mol.

(18) Stein, S. E. *Carbon* **1981**, *19*, 6, 421−429. Stein, S. E.; Brown, R. L. *J. Am. Chem. Soc.* **1991**, *113*, 787−793.

(19) Truhlar, D. G. *J. Comput. Chem.* **1991**, *12*, 266−270.

(20) The second maximum that appears is at r(C−H) = 2.3 Å for the curves at high temperatures (1000 and 1500 K); it is likely due to small errors in the entropic contribution, which are magnified by the term ($T*S$). This error might be caused by the existence of a small (9.05 cm^{-1}) second imaginary frequency.

(21) It should be noted that, at larger distances (>3.5 Å) and also at higher temperatures, the curves show some oscillating behavior.

(22) We used T = 300 K unless mentioned otherwise.

(23) Smith, C. M.; Savage, P. E. *Energy Fuels* **1992**, *6*, 195−202.

(24) The calculated BDE is computed from the BDE of toluene (88 kcal/mol) [McMillen, D. F.; Golden, D. M. *Annu. Rev. Phys. Chem.* **1982**, *33*, 493−532.] and the estimated 5.1 kcal/mol resonance stabilization energy between the 1-methylpyrenyl radical and benzyl radical [Poutsma, M. L. *Energy Fuels* **1990**, *4*, 113−131].

(25) Calculated from Hückel molecular orbital theory: Stein, S. E.; Brown, R. L. *J. Am. Chem. Soc.* **1991**, *113*, 787−793.

(26) The experimental data were obtained from the National Institute for Standards and Technology (NIST): http://kinetics.nist.gov/index.php.

(27) Korobkov, V. Y.; Kalechits, I. V. *Russ. J. Phys. Chem. (Engl. Transl.)* **1991**, *65*, 346−351.

(28) Note that the calculated E and A values are temperature dependent due to the terms containing RT and $R'T$ in eqs II and III.

(29) Muller-Markgraf, W.; Troe, J. *J. Phys. Chem.* **1988**, *92*, 4899.

(30) Baulch, D. L.; Cobos, C. J.; Cox, R. A.; Esser, C.; Frank, P.; Just, Th.; Kerr, J. A.; Pilling, M. J.; Troe, J.; Walker, R. W.; Warnatz, J. *J. Phys. Chem. Ref. Data* **1992**, *21*, 411−429.

(31) Brand, U.; Hippler, H.; Lindemann, L.; Troe, J. *J. Phys. Chem.* **1990**, *94*, 6305.